THE EFFECT OF SOLID BED DISPERSITY ON THE CONTACT HEAT TRANSFER IN ROTARY DRUMS

Nafsun, A.I.[1, 2]* and Herz, F.[1]
*Author for correspondence
[1]Otto von Guericke University Magdeburg, 39106 Magdeburg, Germany
[2]Universiti Malaysia Pahang, Lebuhraya Tun Razak, 26300 Gambang, Kuantan, Pahang, Malaysia
E-mail: aainaa.nafsun@gmail.com

ABSTRACT

Experimental work was conducted to study the influence of bulk bed dispersity on contact heat transfer. The contact heat transfer between the inner drum wall to the covered surface of the solid bed was experimentally investigated in an indirectly heated rotary drum with a diameter of D = 0.6 m and a length of L = 0.45 m. The temperature of the inner drum wall and the solid bed were measured by K-type thermocouples assembled on a rod, upon which these thermocouples were specifically arranged at different radial distances from the inner wall. Experiments have been carried out with glass beads as the test material, with systems defined as monodisperse, bidisperse and polydisperse and with different particle size ratios. The operating parameters, rotational speed and filling degree are varied in the range of 1 to 6 rpm and 10 to 20% respectively. The measured contact heat transfer coefficients for all disperse systems were compared with four model approaches from the literature in terms of R^2 values. Good agreement between the experimental measurements and the two model approaches were achieved.

INTRODUCTION

Rotary drums are processing apparatuses used for drying, calcination or sintering in a variety of industries in order for granular materials to undergo a thermal treatment. The temperature range of these processes extends from 100 to 2000°C. The process in rotary drums depends on operational parameters (rotational speed, filling degree, material throughput and flow rate of gas), heating parameters (type of fuel, flame length and head supply) and design parameters (diameter, length and inclination angle). The interpretation of the process is always based on personnel experience because the interaction between these process parameters is not sufficiently known. Hence, process simulation is necessary for a safe and accurate design of rotary drums and for process optimization. For an adequate process simulation, the heat transfer has to be known. One of the most important heat transfer mechanisms is heat transfer by contact from the covered wall to the covered solid bed. This mechanism is dominant in an indirectly heated rotary drum and contributes up to 20% of the total amount of heat transferred to the solid bed in a directly heated drum [2].

NOMENCLATURE

A_{WS}	[m²]	Contact surface area
$\alpha_{S,penetration}$	[W/m²/K]	Penetration heat transfer coefficient
α_{WP}	[W/m²/K]	Wall-Particle heat transfer coefficient
$\alpha_{WP,rad}$	[W/m²/K]	Radiation heat transfer coefficient
$\alpha_{WS,contact}$	[W/m²/K]	Heat transfer coefficient at the first particle layer
$\alpha_{WS,\lambda}$	[W/m²/K]	Contact heat transfer coefficient
$c_{p,S}$	[J/kg/K]	Solid specific heat capacity
d_P	[m]	Particle diameter
h	[m]	Bed height
L	[m]	Length of the drum
M_S	[kg]	Mass of the solid bed
R	[m]	Drum radius
$t_{contact}$	[s]	Contact time
T	[°C]	Temperature
λ_S	[W/m/K]	Solid bed conductivity
ρ_S	[kg/m³]	Solid bed density

Special characters

μ_P	[-]	Mean roughness on particle surface
F	[%]	Filling degree
l_G	[m]	modified free path of the molecules
n	[rpm]	Rotational speed
s_n	[mm]	Thermocouple distance
γ	[rad]	Filling angle
τ_W	[-]	Coverage factor

Subscripts

G	Gas
P	Particle
S	Solid
S,m	Mean solid bed
W	Wall

Simulation and experimental work on contact heat transfer for a monodisperse system [1, 5-8, 11, 16-18] was done previously. A variety of models [7, 11-13] were developed to describe the contact heat transfer for monodisperse systems. These models show quantitatively significant differences between each other. However, in industrial applications most of the processes in rotary drums involve polydisperse solid beds. A polydisperse system is closely related to product quality issues

since the solid bed tends to segregate and create an inhomogeneous temperature distribution within the bed. Hence, it is crucial to study different disperse systems of solid bed (monodisperse, bidisperse and polydisperse) in order to study the influence on the contact heat transfer coefficient. Furthermore, comparison between some existing models from the literature with the experimental data in terms of R^2 values can demonstrate the best fitting model for all dispersity.

MODELLING OF THE CONTACT HEAT TRANSFER

Heat Transfer Mechanism and Motion Behavior

The heat transfer mechanism in rotary drums involves a combination lots of mechanisms including conduction, convection and radiation. Figure 1 shows the schematic heat transfer in an indirectly heated rotary drum. As the rotary drum wall, which is usually made of steel or graphite, is heated externally with $\dot{Q}_{total}$, heat from the source (electrical, gas, flame) is transported to the wall and then conducted through the wall $\dot{Q}_W$. A part of the heat radiates to the free solid bed surface $\dot{Q}_{WS,\varepsilon}$ and the other part is conducted from the covered wall surface to the solid bed in the contact region, $\dot{Q}_{WS,\lambda}$.

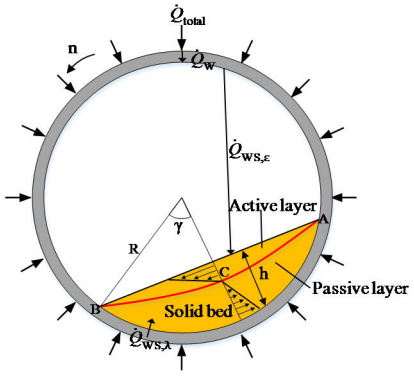

Figure 1 Schematic of the heat transfer in the cross section of indirect heated rotary drums

The covered and free surface of the wall and solid bed depends on the filling degree of the solid bed. The filling degree can be defined as the ratio of the cross sectional area of the solid bed to the total cross sectional area of the drum as shown in Figure 1. The geometric relation can be expressed as

$$F = \frac{A_{solid\ bed}}{A_{drum}} = \frac{\gamma - \sin\gamma\cos\gamma}{\pi} \quad \text{with } \gamma = \arccos\left(1-\frac{h}{R}\right), \qquad (1)$$

with the filling angle γ and the solid bed height h. In rotary drum processes, rolling motion is desirable because it can realize perfect mixing of the solid bed. The motion behavior is influenced by the operational parameters (filling degree and rotational speed), design parameters (diameter and inclination angle) and material parameters. Typically, the filling degree used for industrial applications is in the range of 10% to 20%.

The rolling motion is described by the subdivision of the solid bed into two regions, the passive layer in the lower region and the active layer in the upper region. These layers are separated by a fictitious boundary layer (ACB). In the passive layer, the particles are lifted up to the upper region due to contact with the wall during the rotation of the drum. At the upper boundary line (CA), the particles are mixed up into the active layer and flow downward due to gravity along the line (AB). At the boundary line (BC), particles are mixed out of the active layer and mixed into the passive layer. This process occurs continuously; therefore, the solid bed is well mixed. Extensive experimental studies and modeling of the rolling motion was completed by Henein et al. [3, 4], Liu et al. [14] and Mellmann [15].

Contact Heat Transfer

The contact heat transfer coefficient consists of the serial connection of the contact resistances between the wall and the particles $\alpha_{WS,contact}$ and the penetration coefficient inside the solid bed $\alpha_{S,penetration}$ as described in Schlünder [10].

$$\alpha_{WS,\lambda} = \frac{1}{(1/\alpha_{WS,contact})+(1/\alpha_{S,penetration})} \qquad (2)$$

Due to the contact resistance, a high temperature gradient between the wall and the first particle layer occurs near the wall, while the temperature decreases further into the solid bed because of the heat penetration resistance. By replacing the thermo physical properties of a particle (ρ_P, c_P, λ_P) with the effective properties of a bulk bed (ρ_S, $c_{p,S}$, λ_S), the bed can be regarded as a quasi-continuum and the temperature further into the solid bed is defined as the average bulk temperature. Assuming a constant wall temperature, the penetration coefficient is then obtained from Fourier's differential equation with

$$\alpha_{S,penetration} = 2\sqrt{\frac{\rho_S\, c_{p,S}\, \lambda_S}{\pi t_{contact}}} \qquad t_{contact} = \frac{\gamma}{\pi n}, \qquad (3)$$

where the contact time depends on the filling degree and the rotational speed. A notational gas layer between the first particle layer and the wall surface was assumed, which substantially affected the heat transfer by contact depending on the particle size. Schlünder [9] provided a physical justification for this process. It was expected that, near the point of contact between the particles and the wall, a gas gap occurs in which the mean free path of the gas molecules is always greater than the thickness of this gas gap. Therefore, to compute the contact resistance between the bed and the wall surface, the conduction and radiation in the gas gap between the particles and the wall have to be considered in accordance with

$$\alpha_{WS,contact} = \tau_W \alpha_{WP} + (1 - \tau_W)\frac{2\lambda_G / d_P}{\sqrt{2} + 2(l_G + \mu_P)/d_P} + \alpha_{WP,rad}. \qquad (4)$$

This correlation was given by Schlünder and Mollekopf [11]. The second term in Eq. (4) describes the heat conduction to the second particle layer of the solid bed. The other variables are: α_{WP} and $\alpha_{WP,rad}$, the heat transfer coefficients by conduction and radiation in the gas gap between the first particle layer and the

wall; τ_W the porosity dependent surface coverage factor; λ_G the conductivity of the gas in the gap; d_p the particle diameter; μ_P the mean roughness on the particle surface and l_G the modified free path of the molecules.

Wes et al. [13] investigated the contact heat transfer in an indirectly heated pilot plant (L = 9 m / D = 0.6 m). Within the experimental test series, maximum rotational speeds of n = 6.5 rpm were realized, so that the measurement results could be correlated with the penetration theory according to Eq. (3). Tscheng et al. [12] summarized the results of Wachters and Kramers [16] and Lehmberg et al. [6]. The model by Tscheng et al. [12] used a theory of a fictitious gas film between the wall surface and the first particle layer. A listing of the various models for the contact heat transfer in rotary drums was provided by Li et al. [7]. Furthermore, a simplified model for the contact heat transfer based on [11] was developed.

Herz et al. [5, 17-18] investigated the contact heat transfer in an externally heated batch rotary drum (L=0.45 m / D=0.6 m). The contact heat transfer coefficients were calculated from the temperature measurements and compared with the models by Li et al. [7], Schlünder and Mollekopf [11], Tscheng and Watkinson [12] and Wes et al. [13]. The first attempt was made to investigate the influence of rotational speed and filling degree on contact heat transfer for quartz sand [5]. The results demonstrated that the contact heat transfer coefficients increase with higher rotational speed and lower filling degree. Further investigation was carried out where the results showed that the contact heat transfer decreases with bigger particle size [17]. Copper showed the highest value of contact heat transfer coefficients compared to glass beads and quartz sand. Furthermore, the influence of motion types (sliding, slumping and rolling) on contact heat transfer was examined [18]. The measured contact heat transfer coefficient decreases significantly from rolling to slumping and sliding.

EXPERIMENTS

Experimental Setup and Test Materials

Investigation on the contact heat transfer was done in a batch rotary drum as illustrated in Figure 2. The cylindrical drum was made of stainless steel with a wall thickness of 2 mm, an inner diameter of 600 mm and a length of 450 mm. The drum was partially closed on both sides to prevent spillage of material. It is heated indirectly using three electric heaters with a total capacity of 4.5 kW, sufficient to reach a maximum bed temperature of 200°C. The test material was heated up from ambient temperature to steady-state conditions using a constant heat flux from the outer heating system. The temperature of the inner wall, air and solid bed were measured by thermocouples installed to the drum. The temperature inside the drum was measured by 15 thermocouples attached to a rotating rod at specific distances from the inner drum wall as shown in Figure 3. With this rotating rod, the radial temperature as well as the circumferential temperature profile of the solid bed could be measured simultaneously. In addition, one thermocouple was installed directly on the surface of the inner wall of the drum to simultaneously measure the wall temperature of the drum. Hence, overall 16 thermocouples were used to measure the temperature inside the drum. These thermocouples are Type K thermocouples, made of NiCr-Ni with a diameter of 0.5 mm. Another stationary measuring rod was installed and positioned in the solid bed at a 130° circumferential position. This stationary measuring rod was used to assess the delay of the thermocouples at the rotating rod. Sixteen thermocouples were attached on this rod with the same radial spacing of the rotating rod. The rotating and fixed rods are located at 200 mm and 250 mm in the axial position of the drum respectively. Hence, there is no end wall effect on the contact heat transfer. The temperature difference between the two measuring rods is observed to be negligible. This is because of the very low response time when the diameter of the thermocouples is very small. Therefore, the temperature measured by the rotating thermo elements is considered to have sufficient accuracy for the heat transfer calculation.

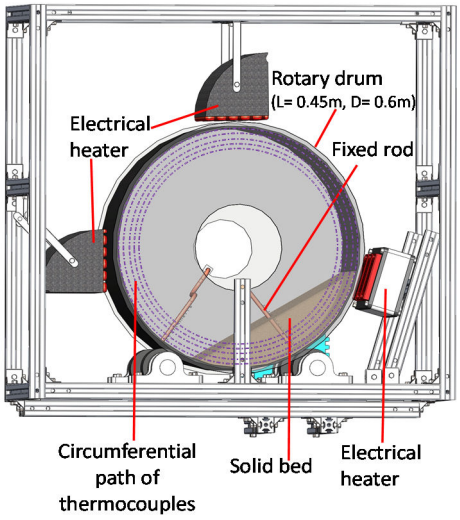

Figure 2 The batch rotary drum for the investigation of contact heat transfer coefficient

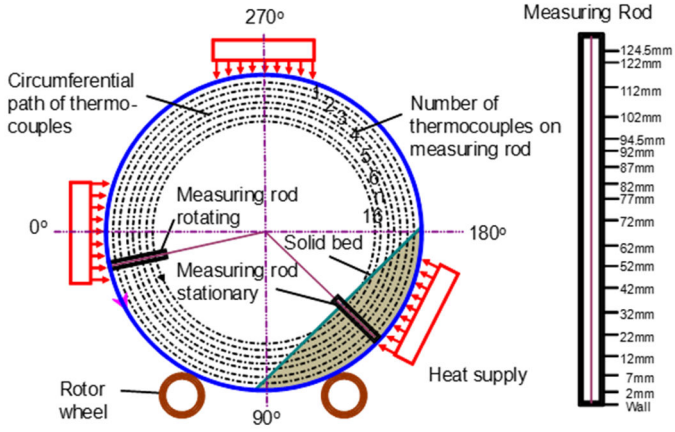

Figure 3 Schematic cross section of the batch rotary drum (left side) and the thermocouples arrangement (right side)

The experiments were performed with filling degrees from 10% to 20% and rotational speeds from 1 rpm to 6 rpm. Glass

beads (d_P = 0.7, 2.0, 3.0, 4.0, 5.0 mm, ρ_S = 1680 kg/m³, $c_{p,S}$ = 800 J/kg/K and λ_S = 0.25 W/m/K) with different dispersity were used as test material.

Experimental Analysis

The measured circumferential temperature profiles for bidisperse glass beads with a filling degree of 10% and a rotational speed of 1 rpm after 30 minutes experimental time are shown in Figure 4. The thermocouples distanced from the wall measured the air temperature inside the rotary drum initially from 0° to 67° (not shown in the figure). After 67°, the thermocouples located nearest to the wall were the first to be immersed into the solid bed and were followed by the next adjacent thermocouples. The rise in temperature was initially recorded by the thermocouple 2 mm from the wall at about 67° while the last thermocouple that recorded a temperature increase was the thermocouple 87 mm from the wall at 89°. Consequently, the farthest thermocouple (87 mm) emerged from the bed first at about 129° while the nearest thermocouple (2 mm) to the wall emerged out of the bed last at about 160°. As seen in Figure 4, a uniform temperature of the solid bed was obtained from 120° to 160°, but the temperature in the solid bed decreases with radial distance from the wall. The difference in the solid bed temperature depends on the radial position, so a surface-related mean temperature is used to calculate the heat transfer coefficient with

$$T_{S,m}=\frac{A_1\left(\frac{T_W+T_1}{2}\right)+A_2\left(\frac{T_1+T_2}{2}\right)+\ldots.+A_n\left(\frac{T_{n-1}+T_n}{2}\right)}{A_1+A_1+\ldots..+A_n} \quad (5)$$

and

$$A_n = 2\,(R_{n-1}-s_n)\,\gamma\,L. \quad (6)$$

The contact heat transfer coefficient from the experimental study can be calculated using the energy balance equation. This was done by assuming that the total energy supplied from the wall was transferred to the solid bed. Heat losses to the surrounding were neglected because the wall temperature was measured directly at the inner wall of the drum. The enthalpy transport in the wall also was neglected due to the small wall thickness of 2 mm. The heat transfer coefficient was derived from the energy balance as follows:

$$\alpha_{WS,\lambda}\,A_{WS}\left(T_W-T_{S,m}\right)=M_S c_{p,S}\frac{dT_{S,m}}{dt} \quad \text{with} \quad A_{WS}=2\gamma RL\,, \quad (7)$$

where $T_{S,m}$ is the mean temperature of the solid bed, T_W is the wall temperature and $c_{p,S}$ is the specific heat capacity of the solid bed. The mass of the solid bed M_S and the contact surface area A_{WS} are dependent on the filling degree and solid material, which do not vary during the test series.

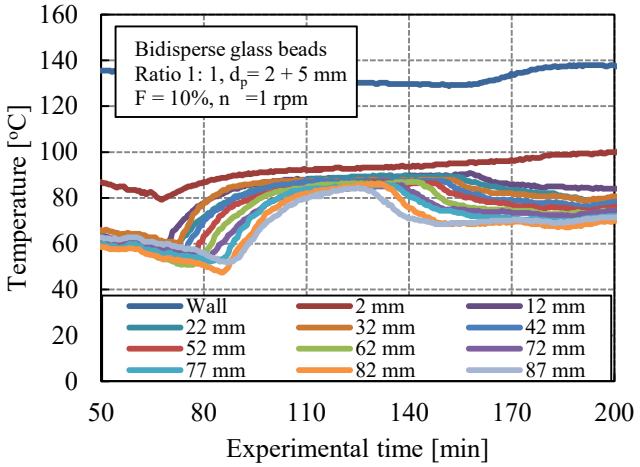

Figure 4 Circumferential temperature profiles of the wall and inside the solid bed.

RESULTS AND DISCUSSION

Figure 5 shows the temperature profiles of the inner drum wall and mean solid bed for bidisperse glass beads with a filling degree of 10% and a rotational speed of 1 rpm during the measurement. Initially, the temperature difference between the inner wall and mean solid bed is relatively large. Then the temperature difference decreases until the value almost reaches steady state at 100 minutes where the mean bed temperature converges to the wall temperature. The temperature gradient in the solid bed also reduces and has a tendency toward zero; hence, the contact heat transfer coefficient decreases.

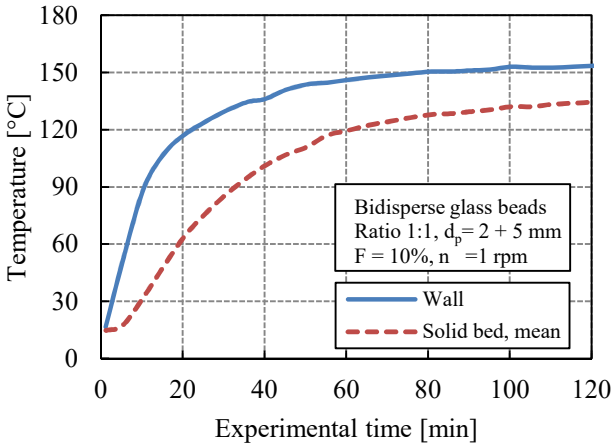

Figure 5 Time curve of the mean solid bed and inner wall temperature during the experiment.

Figure 6 shows the contact heat transfer coefficient for bidisperse glass beads with a filling degree of 10% and a rotational speed of 1 rpm during the experiment. As the contact heat transfer coefficients are derived from the temperature measurement, these values are fluctuating due to the temperature oscillation during the experiment. From these fluctuating values of the heat transfer coefficient, a mean heat transfer coefficient was obtained. The deviation of the regression curve is in the

range of 20%, which is represented by the error bars of the mean values in Figure 6. It can be seen that all the measured values are in the range of accuracy. The regression curve of the mean heat transfer coefficients were also formed for each set of experiments.

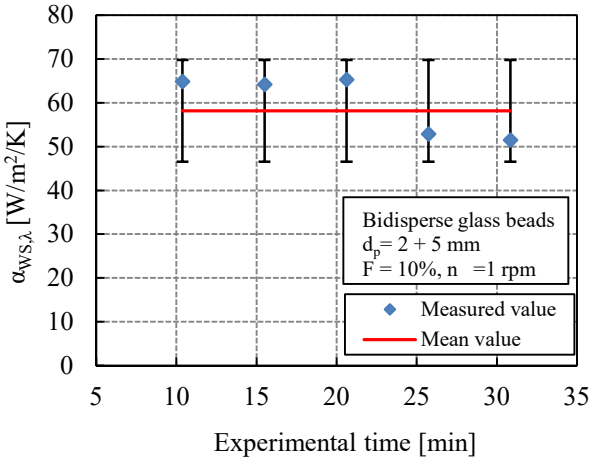

Figure 6 Time curve and regression deviation of the contact heat transfer coefficient during a test section.

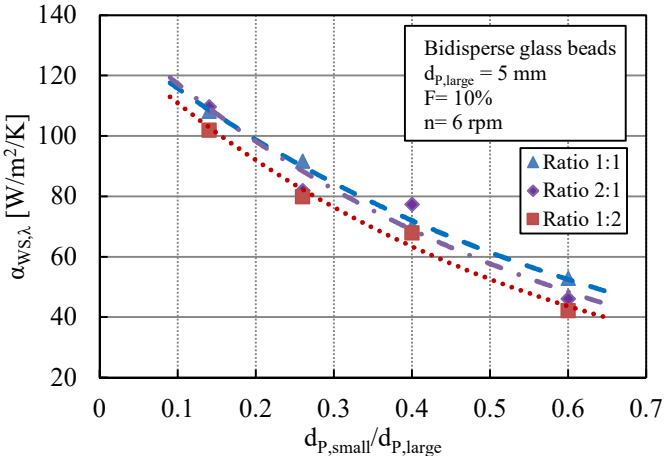

Figure 7 Contact heat transfer coefficient for glass beads in dependence on particle size ratio.

Figure 7 shows the influence of particle size ratio $d_{P,small}/d_{P,large}$ on the contact heat transfer coefficient with a filling degree of F = 10% and a rotational speed of n = 6 rpm for different volume fraction ratios (1:1, 2:1, 1:2). The glass beads with small particle fraction diameters of $d_{P,small}$ = 0.7, 1.3, 2.0 and 3.0 mm were used with the large particle fraction diameter of $d_{P,large}$ = 5 mm as a reference. It is shown that, as the size ratio increases, the contact heat transfer asymptotically decreases and approaches the value for a monodisperse system of the large reference particle diameter ($d_{P,large}$ = 5 mm). Due to bigger particle diameter, the contact resistance between the inner wall and the first particle layer increases, thus reducing the contact heat transfer coefficient. However, the volume fraction ratio does not significantly influence the contact heat transfer coefficient and a clear tendency could not be observed.

The influence of disperse system and the volume ratio of $d_{P,small}/d_{P,large}$ are shown in Figure 8 for a constant rotational speed of F = 10%. The results were shown for bidisperse glass beads consisting of 2 mm and 5 mm particles with ratio of 1:1 , 1:2 and 2:1 and a polydisperse system consist of 0.7, 1.3, 2 and 5 mm with ratio of 1:1:1:1. A higher contact heat transfer coefficient is shown with higher rotational speed due to increase of bed circulation and intensity of mixing as discussed previously by Herz et al. [5,17]. It is clear that with a larger fraction of bigger particles the contact heat transfer coefficients were reduced. This is due to the increase of the contact resistance for bigger particles on the inner wall. The largest heat transfer coefficients are shown for a polydisperse system. Due to the existence of smaller particles (0.7 and 1.3 mm) in the polydisperse system, the contact resistance at the wall decreases, hence larger contact heat transfer coefficients was obtained compared to a bidisperse system for all ratios.

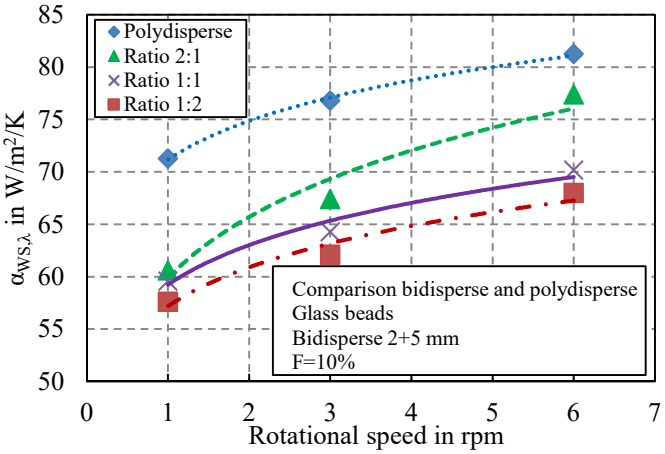

Figure 8 Contact heat transfer coefficient of bi- and polydisperse system as a function of rotational speed.

The measured contact heat transfer coefficients for all disperse systems (monodisperse, bidisperse and polydisperse) were compared with model calculations by Wes et al. [13], Tscheng and Watkinson [12], Schlünder and Mollekopf [11] and Li et al. [7]. The accuracy of model prediction by Wes et al. [13], Tscheng and Watkinson [12], Schlünder and Mollekopf [11] and Li et al. [7] are shown in Figure 9, Figure 10, Figure 11 and Figure 12 respectively. Correlation of model calculation and measured values were represented by the adjusted R^2 values, where a higher R^2 value means better correlation. The model by Wes et al. [13] and Tscheng and Watkinson [12] show low R^2 values (-0.4042 and 0.0975) as shown in Figure 9 and Figure 10 respectively. Large difference between the model calculation of Wes et al. [13] and experimental measurement is due to the fact that the contact resistance between the wall and first particle layer is neglected and the contact heat transfer coefficient is only based on the heat penetration coefficient. The R^2 value for the model by Tscheng and Watkinson [12] is slightly higher than Wes et al. [13]. This is because the authors considered the contact resistance in their model. However, the model could not be well validated with the experimental values because of the

assumption of a fictitious gas film between the wall and the bulk bed, which overestimates the contact resistance.

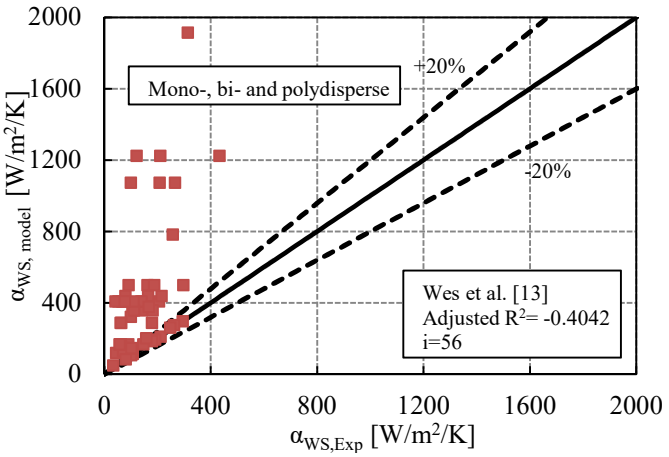

Figure 9 The accuracy of model prediction by Wes et al. [13] for mono-, bi- and polydisperse system.

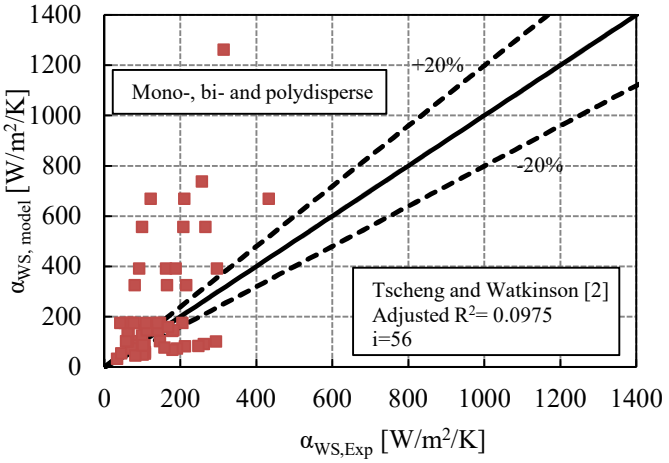

Figure 10 The accuracy of model prediction by Tscheng and Watkinson [12] for mono-, bi- and polydisperse system.

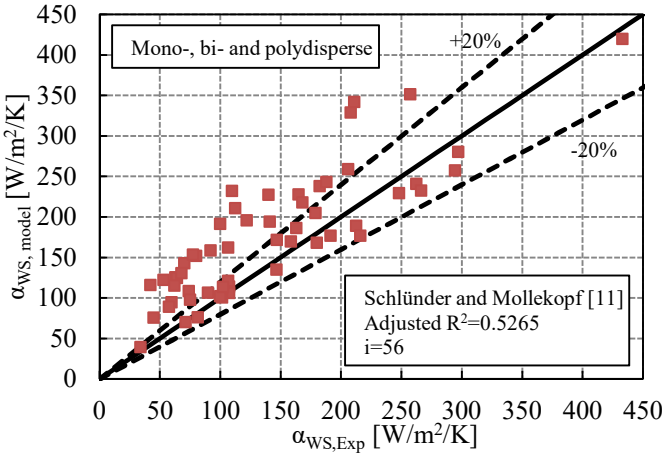

Figure 11 The accuracy of model prediction by Schlünder and Mollekopf [11] for mono-, bi- and polydisperse system.

Good agreement was observed between the model of Schlünder and Mollekopf [11] and Li et al. [7] with the measured values where the R^2 values are 0.5265 and 0.746 respectively. R^2 value for model by Li et al. [7] corresponds to χ value of 0.069, which is defined as the gas film layer thickness. Hence, it can be conclude that the model by Schlünder and Mollekopf [11] and Li et al. [7] is suitable for all disperse systems. The accuracy of the model predictions with experimental results for all the models in terms of R^2 value is summarized in Table 1.

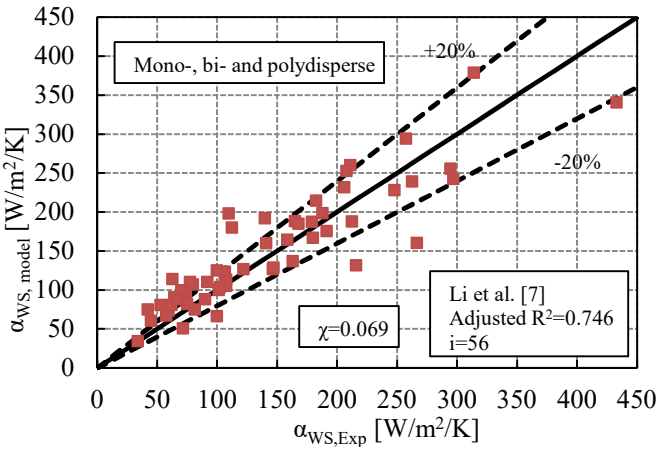

Figure 12 The accuracy of model prediction by Li et al. [7] for mono-, bi- and polydisperse system.

Table 1 Correlation of experimental data with the literature models in terms of R^2 values

Models	R^2 values
Wes et al. [13]	-0.4042
Tscheng and Watkinson [12]	0.0975
Schlünder and Mollekopf [11]	0.5265
Li et al. [7]	0.746

CONCLUSION

The contact heat transfer between the wall and solid bed was experimentally investigated in an indirectly heated rotary batch drum. Glass beads with different disperse systems (mono-, bi- and polydisperse) and particle size ratios were used as test materials with variation in rotational speed and filling degree. It was shown that the contact heat transfer coefficient increases with higher rotational speeds due to higher mixing intensity. Higher particle size ratios leads to lower contact heat transfer because of higher contact resistance between the inner wall and the first particle layer. Furthermore, polydisperse systems show higher contact heat transfer coefficients compare to bidisperse systems. This is due to the presence of smaller particles, hence reducing the contact resistance between the wall and the first particle layer. However, the effect of the dispersity ratio on the contact heat transfer coefficient is small and the tendency is not clear. The measured values were compared with four model

approaches from the literature. The experimental results show good agreement with the model by Schlünder and Mollekopf [11] and Li et al. [7].

ACKNOWLEDGEMENT

The current study has been funded by the German Research Foundation (DFG) within the project SPP 1679 SCHE 322/11-1 and by the German Federation of Industrial Research Associations (AiF) within the project AiF 17133 BG/2. The authors would like to acknowledge this generous support.

REFERENCES

[1] Ernst, R., Heat transfer of heat exchangers in the moving bed, *Chem. Ing. Tech*., Vol. 32, No. 1, 1960, pp. 17-22 (In German).

[2] Gorog, J.P., Adams, T.N. and Brimacombe, J.K., Regenerative heat transfer in rotary kilns, *Metall. Trans. B*, Vol. 13, No. 2, June 1982, pp. 153-163.

[3] Henein, H., Brimacombe, J.K. and Watkinson, A.P., Experimental study of transverse bed motion in rotary kilns, *Metall. Trans. B*, Vol. 14, No. 2, June 1983, pp. 191-205.

[4] Henein, H., Brimacombe, J.K. and Watkinson, A.P., The modeling of transverse solids motion in rotary kilns, *Metall. Trans. B*, Vol. 14, No. 2, June 1983, pp. 207-220.

[5] Herz, F., Mitov, I., Specht, E. and Stanev, R., Experimental study of the contact heat transfer coefficient between the covered wall and the solid bed in rotary drum, *Chemical Engineering Science*, Vol. 82, September 2012, pp. 312-318.

[6] Lehmberg, J., Hehl, M. and Schügerl, K., Transverse mixing and heat transfer in horizontal rotary drum reactors, *Powder Technol.*, Vol. 18, No. 2, November-December 1977, pp. 149-163.

[7] Li, S.-Q., Ma, L.-B., Wan, W. and Yan, Q., A mathematical model of heat transfer in a rotary kiln thermo-reactor, *Chem. Eng. Technol*., Vol. 28, No. 12, December 2005, pp. 1480-1489.

[8] Lybaert, P., Wall-particles heat transfer in rotating heat exchangers, *Int. J. Heat Mass Transfer*, Vol. 30, No. 8, August 1987, pp. 1663-1672.

[9] Schlünder, E.-U., Wärmeübergang an bewegte Kugelschüttungen bei kurzfristigem Kontakt, *Chem. Ing. Tech.*, Vol. 43, No. 11, June 1971, pp. 651-654.

[10] Schlünder, E.-U., Heat transfer to packed and stirred beds from the surface of immersed bodies, *Chem. Eng. Process.*, Vol. 18, No. 1, 1984, pp. 31-53.

[11] Schlünder, E.-U. and Mollekopf, N., Vacuum contact drying of free flowing mechanically agitated particulate material, *Chem. Eng. Process*., Vol. 18, No. 2, March-April 1984, pp. 93-111.

[12] Tscheng, S.H. and Watkinson, A.P., Convective heat transfer in a rotary kiln, *Can. J. Chem. Eng*., Vol. 57, No. 4, August 1979, pp. 433-443.

[13] Wes, G.W.J., Drinkenburg, A.A.H. and Stemerding, S., Heat transfer in a horizontal rotary drum reactor, *Powder Technol*., Vol. 13, No. 2, March-April 1976, pp. 185-192.

[14] Liu, X.Y., Specht, E., Gonzalez, O.G. and P. Walzel, Analytical solution for the rolling mode granular motion in rotary kilns, *Chem. Eng. Process*., Vol. 45, No. 6, June 2006, pp. 515-521.

[15] Mellmann, J., The transverse motion of solids in rotating cylinders-forms of motion and transition behavior, *Powder Technol*., Vol. 118, No. 3, August 2001, pp. 251-270.

[16] Wachters, L.H.J. and Kramers, H., The calcining of sodium bicarbonate in a rotary kiln, *Proceedings of 3rd European Symposium Chemical Reaction Engineering*, Vol. 77, 1964.

[17] Herz, F., Mitov, I., Specht, E., and Stanev, R., Influence of operational parameters and material properties on the contact heat transfer in rotary kilns. *International Journal of Heat and Mass Transfer*, Vol. 55, 2012, pp. 7941-7948.

[18] Herz, F., Mitov, I., Specht, E., and Stanev, R., Influence of the Motion Behavior on the Contact Heat Transfer Between the Covered Wall and Solid Bed in Rotary Kilns. *Experimental Heat Transfer*, Vol. 28(2), 2015, pp.174-188.